REVISTA MATÉRIA V.28 N.3
ISSN 1517-7076 articles e20230176, 2023

A study on the refractive index of sol-gel $Ba_{1-x}Gd_xTiO_3$ thin films using spectroscopic ellipsometry

Ala'eddin A. Saif[1], Yen Chin Teh[2], Prabakaran Poopalan[3]

[1]University of Jeddah, College of Science, Physics department. Jeddah, Saudi Arabia.
[2]Infineon Technologies (Kulim) Sdn Bhd. Kedah, Unit Process Development Engineer. Malaysia.
[3]University Malaysia Perlis, School of Microelectronic Engineering, Pauh Putra Campus, 02600, Arau. Perlis Malaysia.
e-mail: aasaif@uj.edu.sa, yenchinteh@gmail.com, prabakaran@unimap.edu.my

ABSTRACT

$Ba_{1-x}Gd_xTiO_3$ thin films have been fabricated at different Gd^{3+} ionic concentrations, film thicknesses, and annealing temperatures using the sol-gel method. The refractive index of the $Ba_{1-x}Gd_xTiO_3$ films on a silicon substrate is characterized using Spectroscopic Ellipsometry (SE), where the ellipsometry angles Ψ and Δ are fitted very well with the Cauchy dispersion model. The results show that the refractive index at 632.8 nm decreases from 2.18 to 1.892 with the increase of the Gd^{3+} ratio, while it increases with film thickness and annealing temperature. This trend for refractive index variation is explained based on interatomic spacing and density densification of the films. Using Wemple–Di Domenico (WDD) model shows that the dispersion energy increases with film thickness and annealing temperature and decreases with Gd^{3+} doping. The relatively high refractive index of the samples supports the possibility of using $Ba_{1-x}Gd_xTiO_3$ thin films as AR coating for solar cells.

Keywords: $Ba_{1-x}Gd_xTiO_3$; Thin films; Refractive index; Ellipsometry.

1. INTRODUCTION

Antireflection (AR) coatings are considered one of the most effective strategies to minimize optical loss for solar cells as illuminated by solar radiation [1, 2]. Perovskites are promising materials to be used as the active layer in solar cells for those that have a reasonable value of energy bandgap, while using the wide bandgap perovskites type as a top antireflection layer to reduce light reflection and enhance high energy photon absorption [3, 4]. Among perovskites, $BaTiO_3$ has a wide bandgap, high ultraviolet and visible spectrum transparency, and a relatively high refractive index [5]. These characteristics are similar to many antireflection coating oxide materials such as ZnO, ZrO_2, and TiO_2 [3]. This means that $BaTiO_3$ would be an attractive option as an antireflection coating layer for solar cells, enhancing radiation absorption by lowering the incoming light reflection, boosting short circuit current (J_{sc}), and thereby improving the performance of solar cells [6]. The benefit of employing $BaTiO_3$ as an antireflection coating material is because of the wide range of preparation methods, which are generally inexpensive. However, much focus has lately been placed on the advancement of sol-gel technology for producing and characterizing $BaTiO_3$ films over the other techniques. At the same time, the sol-gel approach enables to fabrication of homogeneous large-area films and the easiness of doping [7].

Due to the desirable characteristics of Gd_2O_3, it has been used for various optoelectronic devices [8]. Therefore, it is suggested as a dopant for $BaTiO_3$ in this work. In Gd^{3+} doped $BaTiO_3$, substituting Gd^{3+} ions on the Ba^{2+} or Ti^{3+} site in the crystalline structure is proportional to the doping proportion, thus influencing the material's electrical and optical features [9]. A previous study by our team found that $Ba_{0.9}Gd_{0.1}TiO_3$ has a significant transmittance within the visible spectrum and a relatively high energy band gap [10]. Moreover, it is reported by FASASI *et al.* [11] that Gd^{3+} doped $BaTiO_3$ thin films show a high index of refractive. These properties allow using this composition for antireflection coating for different types of solar cells.

Considering the limited works in the literature concerned with studying the optical properties of Gd^{3+} doped $BaTiO_3$. This work attempts to investigate the impact of Gd^{3+} doping, film thickness, and annealing temperature on the refractive index of $Ba_{1-x}Gd_xTiO_3$. In which films of the $Ba_{1-x}Gd_xTiO_3$ formula at different Gd^{3+} doping concentrations, in addition to films prepared at different thicknesses and annealing temperatures via a sol-gel approach and discuss the refractive index of these films using Spectroscopic Ellipsometry.

Corresponding Author: Ala'eddin A. Saif Received on 12/06/2023 Accepted on 31/07/2023

DOI: https://doi.org/10.1590/1517-7076-RMAT-2023-0176

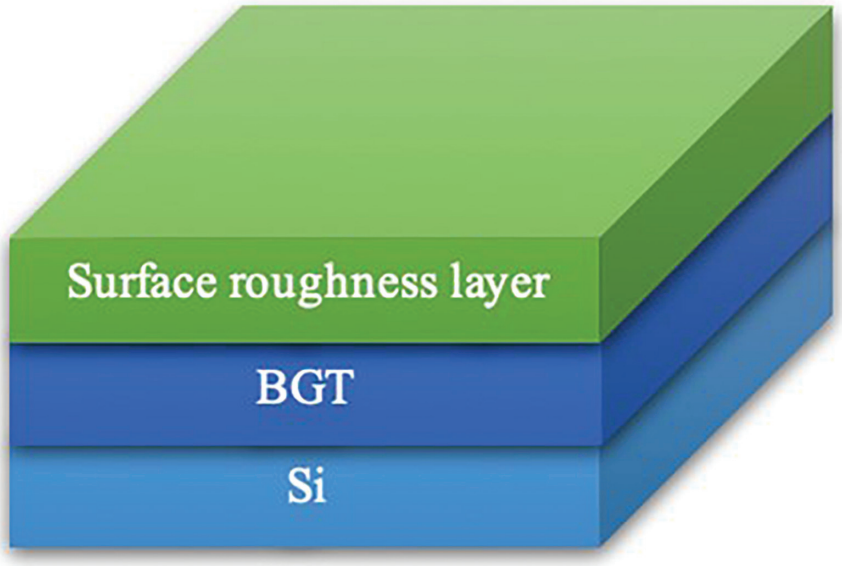

Figure 1: Ellipsometry model for $Ba_{1-x}Gd_xTiO_3$ samples characterization.

2. MATERIALS AND METHODS

$Ba_{1-x}Gd_xTiO_3$ (BGT) thin films with different Gd^{3+} ionic concentrations, thicknesses, and annealing temperatures on Si substrate using the same technique as performed in our previous work [10]. In order to investigate the refractive index of the films, the angle of Psi (Ψ) and Delta (Δ) are recorded using Spectroscopic Ellipsometry (Alpha-SE, J. A. Woollam Co.) within the wavelength range from 381 nm to 893 nm at room temperature. For higher accuracy of the layer modeling, the Ψ and Δ spectra were measured at three different incident angles of 65°, 70°, and 75°. A compatible fitting model built utilizing the BGT/Si sample structure is used to analyze the obtained spectra. A three-layer model structure was proposed to extract the refractive index to fit the measured spectroscopic ellipsometry data [12–14]. Figure 1 illustrates the three-layer model structure used for $Ba_{1-x}Gd_xTiO_3$ films.

3. RESULTS AND DISCUSSIONS

The refractive index of the material beholds a mechanism for trapping the light for more absorption to occur. Theoretically, in the light-to-electricity conversion of photovoltaic applications, a higher refractive index layer adds an advantage to trapping more photons within the material for better absorption. In order to study the refractive index of the $Ba_{1-x}Gd_xTiO_3$ films, the reflectance properties of the films, deposited on a silicon substrate, are studied using Spectroscopic Ellipsometry (SE). In which the polarisation state change of the sample-reflected beam is recorded. The ellipsometric Psi (Ψ) and Delta (Δ) parameters are frequently used to describe the shift in the polarization state; they are usually defined as [15]

$$\rho = \tan(\psi).e^{i\Delta} = \frac{r_p}{r_s} \tag{1}$$

where Ψ and Δ are ellipsometry angles, and r_p and r_s are the complex coefficients of reflection of light that are polarized parallel and normal to the plane of impinging, respectively. Tan Ψ is the ratio of the absolute value of the p-polarized and s-polarized field components, while Δ denotes the phase difference between the reflected components.

The optical model and the best-fit parameter values are calculated using CompleteEASE software provided by J.A. Woollam Co., Inc. The goodness of fitting, denoted as Mean Squared Error (MSE), quantifies the quality of the fitting, and it is defined by [16]

$$MSE = \sqrt{\frac{1}{3n-m}\sum_{i=1}^{n}\left[\left(N_{Ei}-N_{Gi}\right)^2+\left(C_{Ei}-C_{Gi}\right)^2+\left(S_{Ei}-S_{Gi}\right)^2\right]}\times 1000 \tag{2}$$

where *n* is the number of wavelengths, *m* is the number of fitting values, and $N = Cos(2\Psi)$, $C = Sin(2\Psi)Cos(\Delta)$, *and* $S = Sin(2\Psi)Sin(\Delta)$. The data is evaluated using a linear regression technique, and optical parameters and film structures are identified by lowering fitting errors [17]. According to J.A. Woollam Co., the acceptable MSE value should be lower than 20.

The optical constant of $Ba_{1-x}Gd_xTiO_3$ films is derived using a three-layer model (SRL/$Ba_{1-x}Gd_xTiO_3$/ Substrate). Since $Ba_{1-x}Gd_xTiO_3$ films exhibit partial transparency over this wavelength range [10], the measured Ψ and Δ are fitted using the Cauchy dispersion model given by [13]

$$n(\lambda) = A_n + \frac{B_n}{\lambda^2} + \frac{C_n}{\lambda^4} \tag{3}$$

Here, n (λ) represents the refractive index at a specific wavelength λ, whereas A_n, B_n, and C_n are constants. The well-fitted Cauchy dispersion model of the measured Ψ and Δ for $Ba_{1-x}Gd_xTiO_3$ films with various Ba:Gd ratios, film thicknesses, and annealing temperatures are illustrated in Figures 2, 3, and 4, respectively. The figures show the good matching of the fitting model and the measured data with a Mean Squared Error (MSE) value lower than 20. The refractive index dispersion of BGT films is determined through the variable fitted parameters of A_n, B_n, and C_n. The values of the fitted parameters for $Ba_{1-x}Gd_xTiO_3$ films at various Gd^{3+} content, film thicknesses and annealing temperature are summarized in Tables 1, 2, and 3, respectively.

The refractive index dispersion for $Ba_{1-x}Gd_xTiO_3$ films is illustrated in Figure 5. A normal dispersion behavior is observed as the refractive index is reduced with the increase of the wavelength. From Figure 5(a), it is observed that the refractive index at 632.8 nm wavelength reduces from 2.13 to 1.89 with the increase of Gd^{3+} content into the $Ba_{1-x}Gd_xTiO_3$ lattice. The refractive index of polycrystalline films is often controlled by film crystallinity, electronic band structure, lattice point defect, and film density. According to SENGODAN *et al.* [18], the refractive index of the thin film is proportional to electronic polarization, which is also inversely proportional to the interatomic spacing. Interatomic spacing refers to the distance between atoms in the material. When the interatomic spacing reduces and forms packed crystals, the film density increases and thus increases the refractive index as well. Similarly, WANG *et al.* [19] reported that the increase in refractive index is correlated to the expansion of the lattice. This elucidates that the decrease in refractive index is due to the lattice contraction resulting from ionic size reduction. The lattice constants and volume for $Ba_{1-x}Gd_xTiO_3$ are deeply investigated and reported in previous work [20].

The refractive index at different film thicknesses is presented in Figure 5(b). Where the refractive index at 632.8 nm wavelength increases from 2.01 to 2.33 with the increase of film thickness. Generally, the increase in film thickness improves film densification with the addition of layer deposition [13, 21]. Thus, it can be concluded that the variation of the refractive index with the variation of film thickness is attributed to the increase in the film density for thicker films. Under the effect of annealing temperature, the refractive index is increased from 1.76 to 2.12 as the annealing temperature rises from 600 °C to 800 °C. A sudden drop in refractive index to 1.88 is noticed at 900 °C. The increase in refractive index with the annealing temperature is attributed to the improved densification and crystallinity of the films; however, the drop in the refractive index at 900 °C could result from the second phase formed at high annealing temperature [20]. The values of the refractive index for

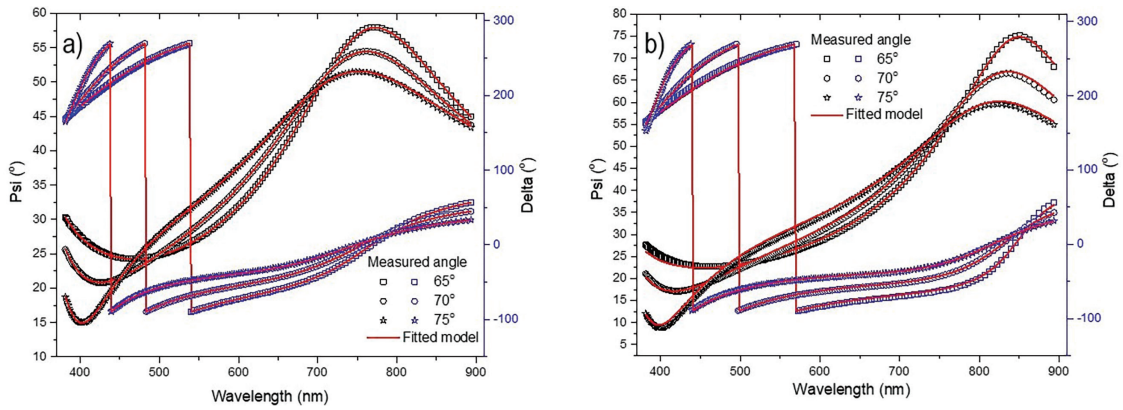

Figure 2: Measured Psi and Delta spectra with the fitted Cauchy model for $Ba_{1-x}Gd_xTiO_3$ films for the ratios (a) 0.95:0.05 and (b) 0.70:0.30.

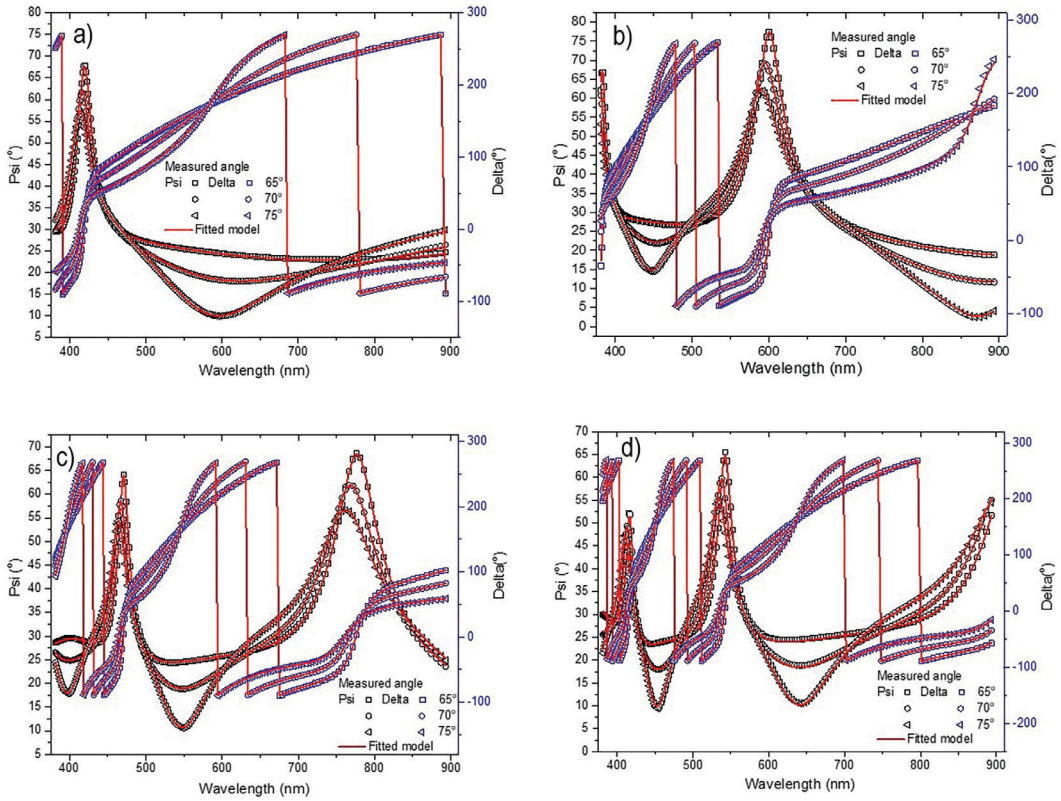

Figure 3: Measured Psi and Delta spectra with the fitted Cauchy model for $Ba_{0.95}Gd_{0.05}TiO_3$ films at various thicknesses (a) 325.56 nm, (b) 424.19 nm, (c) 519.24 nm, and (d) 591.54 nm.

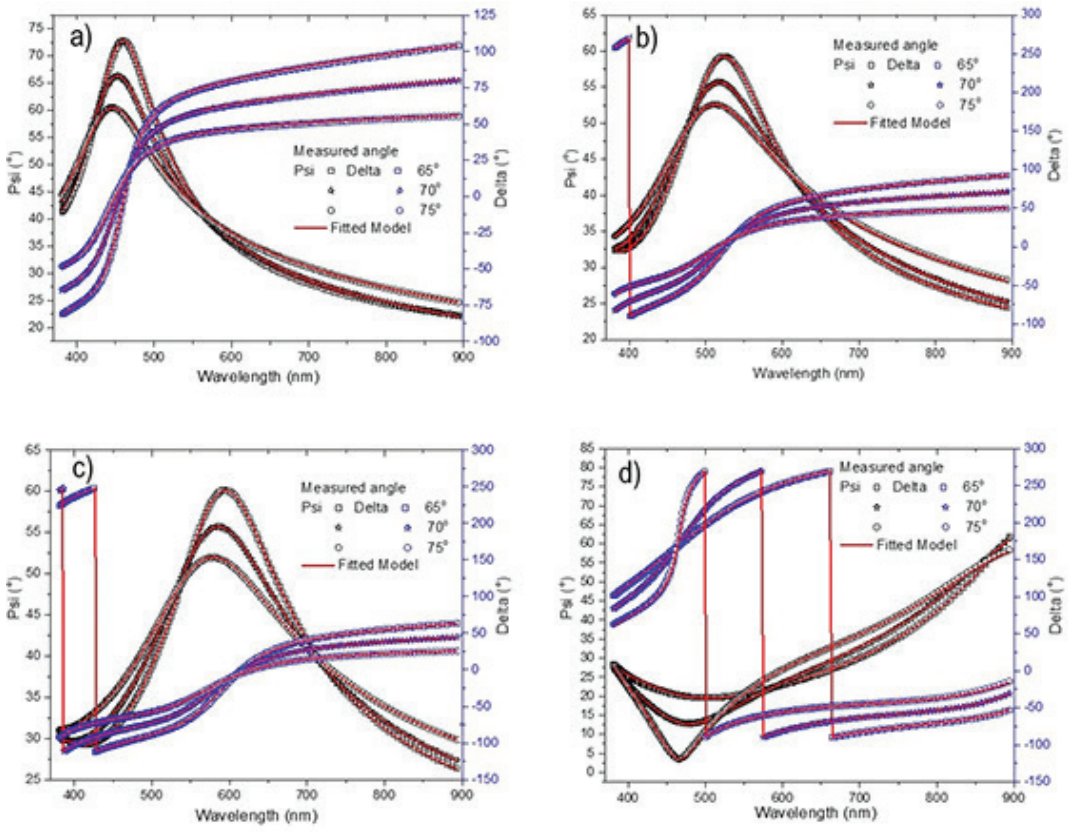

Figure 4: Measured Psi and Delta spectra with the fitted Cauchy model for $Ba_{0.95}Gd_{0.05}TiO_3$ films annealed at (a) 600 °C, (b) 700 °C, (c) 800 °C, and (d) 900 °C.

Table 1: The Cauchy-fitted parameters values for $Ba_{1-x}Gd_xTiO_3$ films at different doping ratios.

Ba:Gd	MSE	A	B (nm^2)	C (nm^4)	n at 632.8 nm
$BaTiO_3$	2.412	2.103 ± 0.253	0.031 ± 0.007	0.0002 ± 0.0001	2.180
0.95:0.05	1.98	2.048 ± 0.232	0.025 ± 0.005	0.0007 ± 0.0002	2.130
0.90:0.10	2.15	2.024 ± 0.221	0.020 ± 0.004	0.0002 ± 0.0001	2.076
0.85:0.15	6.99	1.998 ± 0.889	0.020 ± 0.017	–0.00002 ± 0.0001	2.048
0.80:0.20	1.85	1.926 ± 0.304	0.024 ± 0.008	0.0002 ± 0.0001	1.988
0.75:0.25	2.16	1.887 ± 0.429	0.024 ± 0.011	0.00008 ± 0.0001	1.948
0.70:0.30	13.2	1.847 ± 1.148	0.020 ± 0.026	–0.0008 ± 0.001	1.892

Table 2: The Cauchy-fitted parameters values for $Ba_{0.95}Gd_{0.05}TiO_3$ films at different thicknesses.

THICKNESS (nm)	MSE	A	B (nm^2)	C (nm^4)	n at 632.8 nm
269.57	6.347	1.953 ± 0.528	0.019 ± 0.01	0.00147 ± 0.001	2.008
332.96	8.986	1.971 ± 0.004	0.041 ± 0.002	–0.00046 ± 0.0002	2.071
416.89	10.221	2.204 ± 0.018	0.032 ± 0.01	0.000422 ± 0.001	2.142
502.15	5.487	2.263 ± 0.045	0.016 ± 0.001	0.00447 ± 0.0001	2.332

Table 3: The Cauchy model derived fitted parameters values for $Ba_{0.95}Gd_{0.05}TiO_3$ films at various temperatures.

ANNEALING TEMPERATURE	MSE	A	B (nm^2)	C (nm^4)	n at 632.8 nm
600 °C	7.11	1.718 ± 0.566	0.014 ± 0.011	0.0005 ± 0.0003	1.756
700 °C	3.05	1.874 ± 0.251	0.011 ± 0.003	0.0023 ± 0.0006	1.914
800 °C	2.42	2.068 ± 0.156	0.017 ± 0.002	0.0010 ± 0.0001	2.116
900 °C	5.75	1.864 ± 1.188	0.005 ± 0.007	0.0003 ± 0.0005	1.879

$Ba_{1-x}Gd_xTiO_3$ films show comparable values to the reported refractive index of sol-gel derived BST film [22], BCZT film [19] and $BaTiO_3$ film [12]. However, the values are lower than the reported value for Gd-$BaTiO_3$ film fabricated via laser ablation [11], which could be due to the fabrication method.

In order to have insight into the dispersion of the refractive index of the $Ba_{1-x}Gd_xTiO_3$ films and correlate its behavior with the films' structural order, the refractive index as a function of wavelength is further analyzed by fitting into the Wemple–Di Domenico (WDD) model. The dispersion energy parameters are extracted through the fitting of the WWD model using the following relation [23]

$$n^2 - 1 = \frac{E_0 E_d}{E_0^2 - E^2} \tag{4}$$

where n is the refractive index, E_0 denotes the single-oscillator energy, and E_d denotes the dispersion energy. The dispersion energy describes the average intensity of interband optical transitions and relates to variations in the structural ordering of the material. Figure 6 demonstrates the $1/(n^2–1)$ vs E^2 plot using the least squares fitting of the WWD model. The excellent linear fitting of the straight line in the plot over the wavelength range of 381–893 nm confirms the validity of the WWD model for the $Ba_{1-x}Gd_xTiO_3$ thin films. E_0 and E_d can be evaluated from the slope and the intercept of the plot at $E = 0$. The estimated dispersion energy parameters for $Ba_{1-x}Gd_xTiO_3$ thin films at various Gd^{3+} ratios, film thickness and annealing temperature are listed in Figure 7.

Figure 7(a) illustrates the dispersion energy E_d of $Ba_{1-x}Gd_xTiO_3$ at different Gd^{3+} ratios. It can be noticed that the dispersion energy reduced from 24.99 to 15.13 eV as the Gd^{3+} ratio increased. According to KERMADI *et al.* [24], dispersion energy is related to the structural order of a material. The higher order of the material leads to larger dispersion energy. Accordingly, the decrease in E_d value indicates that the order of the atomic structure

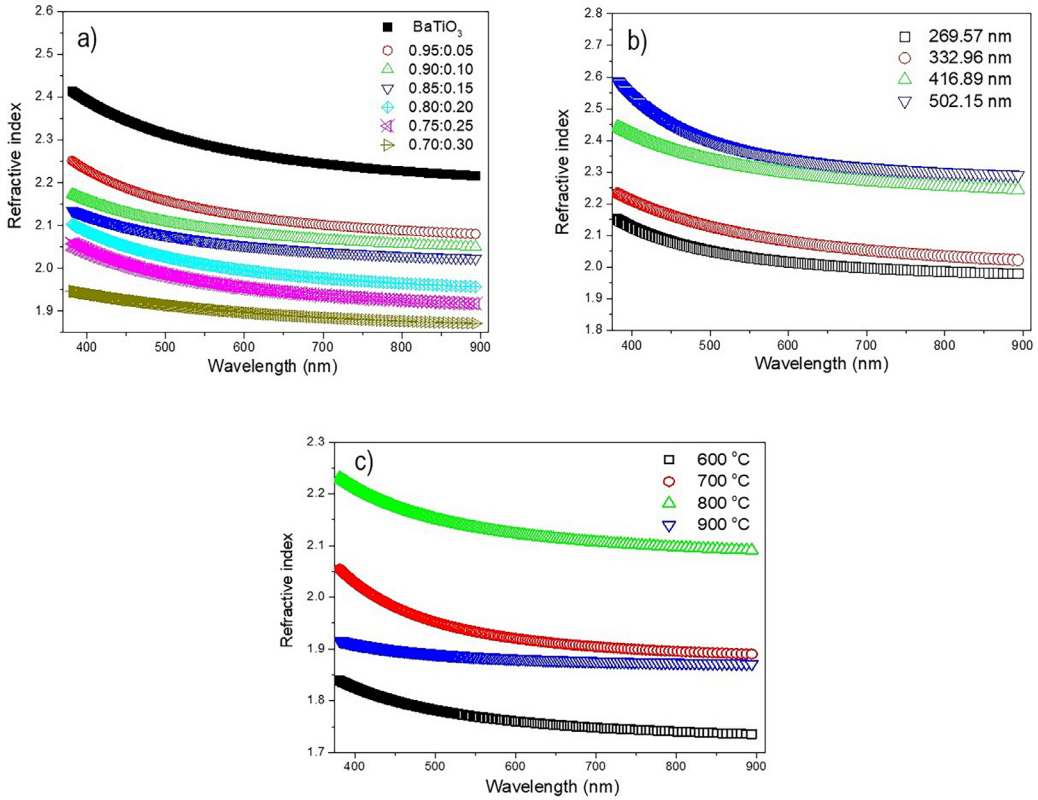

Figure 5: The refractive index dispersion of $Ba_{1-x}Gd_xTiO_3$ thin films at different (a) Ba:Gd ratios, (b) film thicknesses for $Ba_{0.95}Gd_{0.05}TiO_3$, and (c) annealing temperatures.

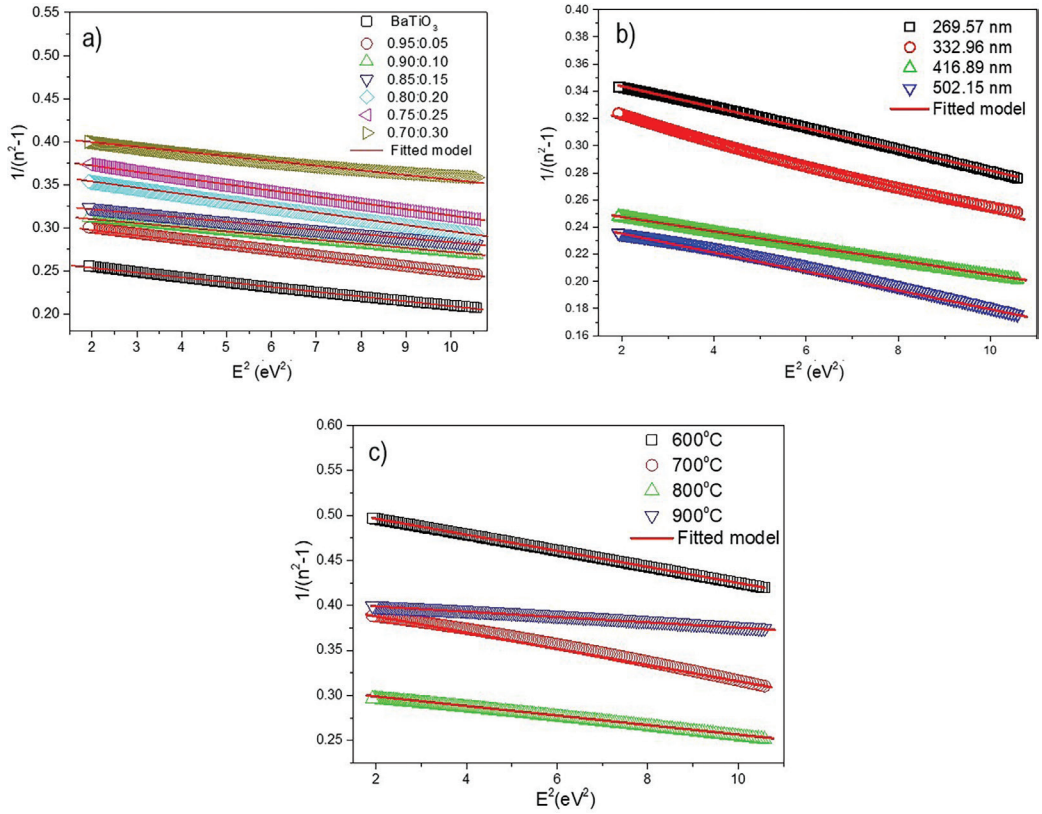

Figure 6: The plot of $(n^2-1)^{-1}$ against E^2 with fitted WWD model for $Ba_{1-x}Gd_xTiO_3$ thin films at different (a) Ba:Gd ratios, (b) thicknesses, and (c) annealing temperatures.

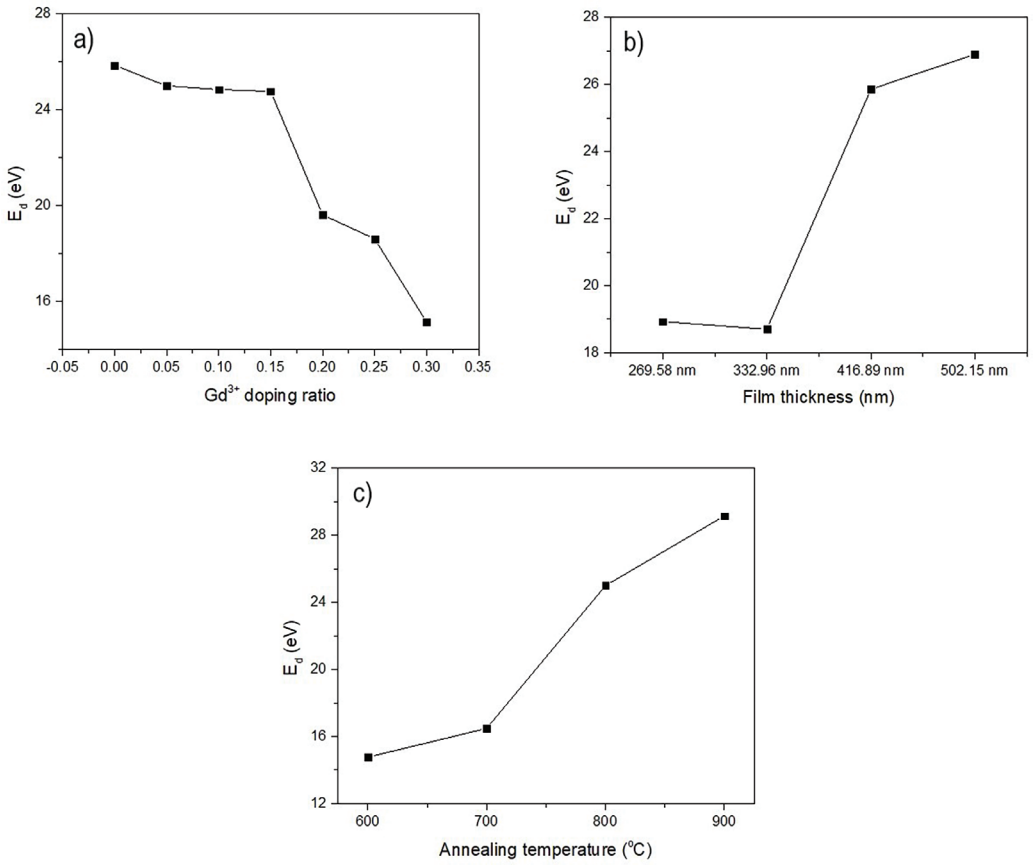

Figure 7: The dispersion energy of $Ba_{1-x}Gd_xTiO_3$ films at various (a) Gd^{3+} doping ratios, (b) film thicknesses, and (c) annealing temperatures.

in the $Ba_xGd_{1-x}TiO_3$ films reduces as more Gd^3 ions are substituted into the Ba-site. To confirm this finding and give detailed information on the level of structural disorder of current films, XRD results from previous work have been employed [20]. In which the estimated lattice constants and volume show decrement variation with Gd^{3+}, indicating that the lattice order is degraded; this is in line with E_d values reduction. A similar observation for the dependence of the dispersion energy on the lattice size for barium strontium titanate films is reported by SINGH *et al.* [25].

An increment in the dispersion energy parameters is observed with the film thickness, as shown in Figure 7(b). The E_d increases from 18.93 to 26.90 eV with the increase of the film thickness, indicating that the microstructure ordering is enhanced. Such increment in the structural order is correlated to the increases in grain size with thickness [20].

Figure 7(c) shows that the strength of dispersion energy E_d increases from 14.77 eV to 29.15 eV with the increase of annealing temperature. When the annealing temperature increased, the order of the atomic structure of the film increased and resulted in high dispersion energy. This is in line with the XRD results reported in a previous work [10], in which it is found that the lattice volume increases with annealing temperature due to lattice growth at higher temperatures, which indicates the crystallinity improvement. Similar behaviour of dispersion energy under the effect of annealing temperature is also observed by Kuo and Tseng in barium strontium titanate thin films [26]. They explained that the increment of the dispersion energy is associated with the increase in film packing density.

4. CONCLUSIONS

The refractive index of $Ba_{1-x}Gd_xTiO_3$ thin films at different Gd^{3+} contents, film thicknesses, and annealing temperatures using Spectroscopic Ellipsometry. The measured Ψ and Δ for all tested samples fitted very well with the Cauchy dispersion model, which is used to evaluate the refractive index of the films. The results show that the dispersion of refractive index with wavelength shows that n at 632.8 nm decreases from 2.18 to 1.892 with the increase of Gd^{3+} ratio, while it increases from 2.01 to 2.33 with film thickness and increases from 1.76 at

600 °C to 2.12 at 800 °C then drops to 1.88 at 900 °C. This trend for refractive index variation is explained based on interatomic spacing and lattice volume. Besides, the films under investigation show very good fitting to the Wemple–Di Domenico (WDD) model; accordingly, the dispersion energy shows an increment with film thickness and annealing temperature, indicating that the microstructure of the films is getting more order. On the other hand, an opposite attitude with Gd^{3+} doping is obtained. Out of the results, it can be concluded that a low Gd^{3+} doping and high film thickness and annealing temperature of 800 °C are recommended to obtain a high value of the refractive index for $Ba_{1-x}Gd_xTiO_3$ thin films for AR coating solar cells application.

5. BIBLIOGRAPHY

[1] JI, C., LIU, W., BAO, Y., *et al*., "Recent applications of antireflection coatings in solar cells", *Photonics*, v. 9, n. 12, pp. 906, Nov. 2022. doi: http://dx.doi.org/10.3390/photonics9120906.

[2] SAIF, A.A. "High-efficiency homojunction GaAs solar cell using InGaP as FSF and AlGaInP as BSF", *Results in Optics*, v. 12, n. 100454, Jul. 2023. doi: http://dx.doi.org/10.1016/j.rio.2023.100454.

[3] SCHOLTZ, L., ŠUTTA, P., CALTA, P., *et al*., "Investigation of barium titanate thin films as simple antireflection coatings for solar cells", *Applied Surface Science*, v. 461, pp. 249–254, Dec. 2018. doi: http://dx.doi.org/10.1016/j.apsusc.2018.06.226.

[4] CHEN, H., XIE, C., ZHONG, X., *et al*., "A quasi-2D perovskite antireflection coating to boost the performance of multilayered $PdTe_2$/Ge heterostructure-based near-infrared photodetectors", *Journal of Materials Chemistry. C, Materials for Optical and Electronic Devices*, v. 10, n. 15, pp. 6025–6035, Mar. 2022. doi: http://dx.doi.org/10.1039/D2TC00438K.

[5] MANEESHYA, L.V., ANITHA, V.S., THOMAS, P.V., *et al*., "Thickness dependence of structural, optical and luminescence properties of $BaTiO_3$ thin films prepared by RF magnetron sputtering", *Journal of Materials Science Materials in Electronics*, v. 26, n. 5, pp. 2947–2954, May. 2015. doi: http://dx.doi.org/10.1007/s10854-015-2781-1.

[6] PARK, H., SHIN, M., KIM, H., *et al*., "Investigation of 3-dimensional structural morphology for enhancing light trapping with control of surface haze", *Optical Materials*, v. 66, pp. 404–409, Apr. 2017. doi: http://dx.doi.org/10.1016/j.optmat.2017.02.039.

[7] LI, J., INUKAI, K., TAKAHASHI, Y., *et al*., "Thin film coating with highly dispersible barium titanate-polyvinylpyrrolidone nanoparticles", *Materials (Basel)*, v. 11, n. 5, pp. 712, May 2018. doi: http://dx.doi.org/10.3390/ma11050712. PubMed PMID: 29724007.

[8] KUZNETSOVA, Y.A., ZATSEPIN, A.F., "Optical properties and energy parameters of Gd_2O_3 and Gd_2O_3:Er nanoparticles", *Journal of Physics: Conference Series*, v. 917, n. 062001, pp. 062001, 2017. doi: http://dx.doi.org/10.1088/1742-6596/917/6/062001.

[9] HAN-SOL, Y., JAE-HYEON, S., YONG-SEON, K., *et al*., "Structural and chemical features of Gd:$BaTiO_3$ solid solutions prepared by microwave-assisted heat treatment", *Bulletin of Materials Science*, v. 44, pp. 241, Sep. 2021.

[10] TEH, Y.C., SAIF, A.A. "Influence of annealing temperature on structural and optical properties of sol-gel derived $Ba_{0.9}Gd_{0.1}TiO_3$ thin films for optoelectronics", *Journal of Alloys Compounds*, v. 703, pp. 407–413, May. 2017. doi: http://dx.doi.org/10.1016/j.jallcom.2017.01.312.

[11] FASASI, A.Y., NGOM, B.D., KANA-KANA, J.B., *et al*., "Synthesis and characterisation of Gd-doped $BaTiO_3$ thin films prepared by laser ablation for optoelectronic applications", *Journal of Physics and Chemistry of Solids*, v. 70, n. 10, pp. 1322–1329, Oct. 2009. doi: http://dx.doi.org/10.1016/j.jpcs.2009.06.022.

[12] HU, Z.G., LI, Y.W., ZHU, M., *et al*., "Microstructural and optical investigations of sol-gel derived ferroelectric $BaTiO_3$ nanocrystalline films determined by spectroscopic ellipsometry", *Physics Letters. [Part A]*, v. 372, n. 29, pp. 4521–4526, Jun. 2008. doi: http://dx.doi.org/10.1016/j.physleta.2008.04.001.

[13] MOHAMED, S.H., DUGHAISH, Z.H., "Microstructural and optical investigations of Ce-doped barium titanate thin films by FTIR and spectroscopic ellipsometry", *Philosophical Magazine*, v. 92, n. 10, pp. 1212–1222, Jan. 2012. doi: http://dx.doi.org/10.1080/14786435.2011.642320.

[14] ZHANG, Y., JIE, W.J., CHEN, P., *et al*., "Ferroelectric and piezoelectric effects on the optical process in advanced materials and devices", *Advanced Materials*, v. 30, n. 34, pp. e1707007, Aug. 2018. doi: http://dx.doi.org/10.1002/adma.201707007. PubMed PMID: 29888451.

[15] MCILLON-BROWN, L., BORDEENITHIKASEM, P., PINNOCK, F., *et al.* "Measured optical constants of $Pd_{77.5}Cu_6Si_{16.5}$ bulk metallic glass", *Optical Materials X*, v. 1, n. 100012, Jan. 2019.

[16] WROBLEWSKI, G., SWATOWSKA, B., DYBOWSKA-SARAPUK, L., *et al*., "Optical properties of transparent electrodes based on carbon nanotubes and graphene platelets", *Journal of Materials Science Materials in Electronics*, v. 27, n. 12, pp. 12764–12771, Jul. 2016. doi: http://dx.doi.org/10.1007/s10854-016-5408-2.

[17] PASCU, R., DINESCU, M., "Spectroscopic ellipsometry", *Romanian Reports in Physics*, v. 64, n. 1, pp. 135–142, 2012.

[18] SENGODAN, R., BELLAN, C., RAJAMANICKAM, B., *et al*., "Temperature dependence of optical properties on $BaTiO_3$ thin films for optoelectronics applications", *Journal of Optoelectronics and Advanced Materials*, v. 19, n. 9-10, pp. 595–603, Sep-Oct. 2017.

[19] WANG, H., XU, J., MA, C., *et al*., "Spectroscopic ellipsometry study of $0.5BaZr_{0.2}Ti_{0.8}O_{3-0.5}Ba_{0.7}Ca_{0.3}TiO_3$ ferroelectric thin films", *Journal of Alloys and Compounds*, v. 615, pp. 526–530, Dec. 2014. doi: http://dx.doi.org/10.1016/j.jallcom.2014.06.186.

[20] SAIF, A.A., TEH, Y.C. "Correlation of Ba:Gd ratio and film thickness to the dielectric, ferroelectric and leakage current mechanism of nanostructure $Ba_{1-x}Gd_xTiO_3$ thin films", *Physica B: Condensed Matters*, v. 612, n. 412824, Jul. 2021. doi: http://dx.doi.org/10.1016/j.physb.2021.412824.

[21] MOLINA, E.F., ROCHA, L.A., CAETANO, B.L., *et al*., "Preparation and study of the titanium oxide thin films doped with Tb3+ and Ce3+ ions", *Matéria (Rio de Janeiro)*, v. 17, n. 1, pp. 931–938, 2012. doi: http://dx.doi.org/10.1590/S1517-70762012000100006.

[22] TIAN, H.Y., LUO, W.G., DING, A.L., *et al*., "Influences of annealing temperature on the optical and structural properties of $(Ba,Sr)TiO_3$ thin films derived from sol-gel technique", *Thin Solid Films*, v. 408, n. 1–2, pp. 200–205, Apr. 2002. doi: http://dx.doi.org/10.1016/S0040-6090(02)00046-9.

[23] SHAABAN, E.R., SORAYA, M.M., SAMAR, M.M., *et al*. "Effects on the linear and nonlinear optical properties of Se-S-Sb chalcogenide glass thin films", *International Journal of Thin Film Science and Technology*, v. 8, n. 3, pp. 175–187, Sep. 2019.

[24] KERMADI, S., AGOUDJIL, N., SALI, S., *et al*., "Microstructure and optical dispersion characterization of nanocomposite sol-gel TiO_2-SiO_2 thin films with different compositions", *Spectrochimica Acta. Part A: Molecular and Biomolecular Spectroscopy*, v. 145, pp. 145–154, Jun. 2015. doi: http://dx.doi.org/10.1016/j.saa.2015.02.110. PubMed PMID: 25770938.

[25] SINGH, S.B., SHARMA, H.B., SARMA, H.N.K., *et al*., "Influence of crystallization on the spectral features of nano-sized ferroelectric barium strontium titanate ($Ba_{0.7}Sr_{0.3}TiO_3$) thin films", *Physica B, Condensed Matter*, v. 403, n. 17, pp. 2678–2683, Aug. 2008. doi: http://dx.doi.org/10.1016/j.physb.2008.01.036.

[26] KUO, Y., TSENG, T., "Structure-related optical properties of rapid thermally annealed $Ba_{0.7}Sr_{0.3}TiO_3$ thin films", *Materials Chemistry and Physics*, v. 61, n. 3, pp. 244–250, Nov. 1999. doi: http://dx.doi.org/10.1016/S0254-0584(99)00157-1.